ECE APPLIED TO ENERGY FROM SPACE-TIME: AMPLIFICATION OF THE RADIATIVE CORRECTION BY SPIN CONNECTION RESONANCE.

by

Myron W. Evans,

Civil List Scientist,

and

H. Eckardt and G. J. Evans,

A.I.A.S.

(Contact: emyrone@aol.com, www.aias.us)

ABSTRACT

The well known radiative correction is amplified by spin connection resonance, whereby the initially Coulombic potential in an easily ionized material is amplified to the point where electrons are released for use in circuits, energy production and energy savings. It is assumed that the radiative correction can be represented by an oscillating part of the fine structure constant. The methods of Einstein Cartan Evans (ECE) field theory are used to amplify the induced jitterbugging of the electron in each orbital that is the primary characteristic of the radiative correction. The latter is observed in well known phenomena such as the electron g factor, the Lamb shift and the Casimir effect. It is shown that the initially small radiative correction can be amplified for practical implementation.

Keywords: Einstein Cartan Evans (ECE) field theory, radiative correction, spin connection resonance amplification, new sources of energy.

Paper 87 of ECE Series

1 INTRODUCTION

Recently the Einstein Cartan Evans (ECE) field theory has offered a generally covariant unified field theory based on the principles of relativity - that physics is objective and causal {1-11}. Relativity is the most precise theory of physics. Electrodynamics and quantum mechanics have been forged together with gravitation and the other fundamental force fields in one theoretical framework based on Cartan geometry {12}. With these developments came the realization that the spin connection of space-time plays a central role in electrodynamics, which in ECE is considered to be a theory of general relativity, not of special relativity. It has been shown {11} that the spin connection can produce amplification of gravitational effects, an amplification which may be used in counter-gravitational devices. In the field of electrodynamics it has been shown {1-11} that the spin connection may be used to amplify the repulsion between electrons in an atom or molecule to the point at which the electrons are freed from the nucleus and may be used in circuits to produce power or save power. Recently, it has been shown {1-11} that the Lamb shift may be explained within experimental precision by using an average effect of the ubiquitous zero'th eigenstate of the quantized electromagnetic field ("zero point energy") to describe the well known {13,14} radiative correction. The Lamb shift has been described in ECE theory in a manner that is consistent with the description of the g factor of the electron in earlier work {1-11}.

In Section 2 the radiative correction in the hydrogen atom is considered to arise from an oscillating component of the averaged radiative correction used in previous work {1-11}. The Lamb shift is illustrated in atomic hydrogen for this type of radiative correction. The charge density in each orbital is calculated for each orbital. In Section 3 these charge densities are used in the generally covariant Coulomb law of ECE theory and it is shown that the radiative correction in each orbital of atomic hydrogen can be amplified by spin connection resonance to the point at which the electron breaks free from the proton and may be used in a

circuit to produce power. This process is known as "energy from space-time". This paper therefore identifies the driving term of the spin connection resonance mechanism as the radiative correction. The latter causes zwitterbewegung, the well known {15} jitterbugging of the electron in each orbital due to the ubiquitous, background, radiative correction. The latter is due to the fact that in the quantized electromagnetic field surrounding the atom, there are ever present and ever oscillating electric and magnetic fields. In the zero'th eigenstate of the quantized, background, electromagnetic field these electric and magnetic fluctuations exist when there are no photons {15} present, the photon being defined as the quantum of energy. The electromagnetic potential due to these fluctuating electric and magnetic fields produces well known phenomena such as the g factor of the electron and other particles, the Lamb shift, and the Casimir effect. These are examples of the ways in which the radiative correction is observed experimentally. No energy is required to manufacture the potential of the radiative correction, which is therefore like an enormous natural reservoir of energy, one which is ever present. The natural effect of the radiative correction is very small (about four parts in ten million ~~of~~ for atomic hydrogen), but in ECE theory (generally covariant unified field theory) it may be amplified by spin connection resonance {1-11}. In Section 4 the results of Sections 2 and 3 are developed numerically, and in Section 5 a discussion is given of the type of material most likely to release electrons through the theory of this paper. The hydrogen atom is used as a model for future work based on density functional code in solids.

2. RADIATIVE CORRECTION IN THE HYDROGEN ATOM.

In previous work on the electron g factor and Lamb shift {1-11} the mean value of the radiative correction was implemented as follows:

$$g \rightarrow g\left(1 + \frac{\langle \alpha \rangle}{4\pi}\right)^2 \quad - (1)$$

$$\nabla^2 \rightarrow \nabla^2 \left(1 + \frac{\langle \alpha \rangle}{4\pi} \right)^2 \quad - (2)$$

where g is the electron g factor, and where α is the fine structure constant. Eq. (1) was used with the Dirac equation derived from the ECE wave equation, and Eq. (2) was used with the Schrödinger equation. In order to model the jitterbugging of the electron it is assumed that:

$$\alpha = \langle \alpha \rangle \left(1 + \cos(\kappa r) \right) \quad - (3)$$

where κ is a characteristic wave-number of the jitterbugging and where r is the radial coordinate {1-11}. The jitterbugging is therefore the initially small driving term of the spin connection resonance (SCR) mechanism of previous work {1-11}. The hydrogen atom is used to model the effect of Eq. (3) on each orbital.

To first order in α :

$$\left(1 + \frac{\alpha}{4\pi} \right)^2 \sim 1 + \frac{\alpha}{2\pi} = 1 + \frac{\langle \alpha \rangle}{2\pi} \left(1 + \cos(\kappa r) \right) \quad - (4)$$

and the Schrödinger equation of atomic hydrogen becomes:

$$-\frac{\hbar^2}{2m} \left(1 + \frac{\langle \alpha \rangle}{2\pi} \left(1 + \cos(\kappa r) \right) \right) \nabla^2 \psi + V^{(0)} \psi = E \psi \quad - (5)$$

where

$$V^{(0)} = -\frac{e^2}{4\pi \epsilon_0 r} \quad - (6)$$

is the initially Coulombic attraction between the proton and electron. The effect of SCR is to amplify this attraction into a strong repulsion which allows the electron to break free from the proton. In Eq. (5), ψ is the wave-function and E is the total energy {15}. In Eq. (6), e

is the charge on the proton (minus the charge on the electron), and ϵ_0 is the vacuum permittivity in S.I. units {15}.

It is well known {15} that Eq. (5) can be developed into:

$$-\frac{\hbar^2}{2m}\left(1+\frac{\alpha}{2\pi}\right)\frac{d^2\rho}{dr^2}+V_{eff}^{(0)}\rho=E\rho \quad -(7)$$

where:

$$\rho(r)=rR(r). \quad -(8)$$

Here R is the radial wave-function of the hydrogen atom. The potential energy in Eq. (7) is

$$V_{eff}^{(0)}=-\frac{e^2}{4\pi\epsilon_0 r}+\frac{l(l+1)\hbar^2}{2mr^2} \quad -(9)$$

where l is the angular momentum quantum number, m is the mass of the electron and $\hbar$ is the reduced Planck constant. The positive term in Eq. (9) is the well known centrifugal repulsion term in atomic hydrogen {15}. Using previous work {1-11} on the Lamb shift in atomic hydrogen and helium, Eq. (7) is re-written as:

$$-\frac{\hbar^2}{2m}\frac{d^2\rho}{dr^2}+V_{eff}\rho=E\rho \quad -(10)$$

$$-(11)$$

where:

$$V_{eff}=-\frac{e^2}{4\pi\epsilon_0(r+r(vac))}+\frac{l(l+1)\hbar^2}{2m(r+r(vac))^2}.$$

Here r(vac) is a radial adjustment due to the radiative correction. It is different for each orbital and can be calculated by subtracting Eq. (10) from Eq. (7), giving:

$$-\frac{\hbar^2}{4\pi m}\alpha\frac{d^2P}{dr^2}+\left(\bar{V}_{eff}^{(6)}-\bar{V}_{eff}\right)P=0. \quad -(12)$$

The known hydrogenic P may be used in Eq. (12) to compute r(vac) using computer algebra. This assumption is based on the experimental fact that the Lamb shift for atomic H splits the 2s and 2p levels by about four parts in ten million, so the hydrogenic wave-functions are only slightly affected. In previous work the experimentally measured Lamb shift was explained in terms of an average r(vac) for the hydrogen and helium atoms. More accurately, as in this paper, r(vac) oscillates from Eq. (3), i.e. the electron jitterbugs in each orbital. The jitterbugging is the phenomenon used to build up the driving term of the SCR mechanism.

To construct the driving term, the charge density ρ in each orbital must be calculated, the driving term is then $-\rho/\epsilon_0$. In order to calculate ρ, it is necessary to calculate the probability of finding the electron in a volume element $d\tau$ at some point (r, θ, ϕ) in spherical polar coordinates {15}. This probability is:

$$dp_e = |\psi(r, \theta, \phi)|^2 d\tau. \quad -(13)$$

The volume element is:

$$d\tau = r^2 dr \sin\theta \, d\theta \, d\phi. \quad -(14)$$

The probability of finding the electron in a spherical shell of thickness dr and radius r is the sum over these probabilities {15} as θ and ϕ move over the range:

$$0 \leq \theta \leq \pi, \quad 0 \leq \phi \leq 2\pi. \quad -(15)$$

This sum is:

$$P_e = \int_0^{\pi} \sin\theta \, d\theta \int_0^{2\pi} |\psi(r,\theta,\phi)|^2 \, d\phi \, dr. \qquad -(16)$$

However, the P function of Eq. (7) depends only on r, so the summed probability is:

$$P_e = 4\pi r^2 P. \qquad -(17)$$

If we consider the probability to be determined by R itself, rather than P, then the summed probability is:

$$P_e = 4\pi r^2 R. \qquad -(18)$$

The use of Eq. (17) or (18) is a matter of choice. If we choose Eq. (18) and normalize the summed probability to be unit-less by use of the Bohr radius a_o {15} we obtain:

$$P_{e,norm} = 4\pi \left(\frac{r + r(vac)}{a_o} \right)^2 R^2. \qquad -(19)$$

This expression has assumed that R is hydrogenic, and unaffected by r(vac), so the latter appears only in the pre-multiplying factor. This is an approximation, but in the hydrogen atom an excellent approximation. In other materials it may not be as good an approximation, and Eq. (5) would have to be solved directly with density functional code or another suitable numerical method. Finally the charge density of each orbital is defined to be:

$$\rho = e P_{e,norm} / V_e \qquad -(20)$$

where V_e is an effective volume for each orbital. If a spherical volume is assumed:

$$V_e = \frac{4}{3} \pi r_e^3 \qquad -(21)$$

where r is the mean radius of each orbital.
e

3. SCR AMPLIFICATION MECHANISM.

This mechanism {1-11} is based on a simplified definition of the electric field in ECE theory:

$$\underline{E} = -\left(\underline{\nabla} + \underline{\omega}\right)\phi \quad -(22)$$

where $\underline{\omega}$ is the spin connection vector and ϕ is the scalar potential. A simplified form of the Coulomb law of ECE theory is used. This happens to have the same mathematical form as the Coulomb law of Maxwell Heaviside theory:

$$\underline{\nabla} \cdot \underline{E} = \frac{\rho}{\epsilon_0} . \quad -(23)$$

The spin connection is assumed to be {1-11}:

$$\omega_r = -\frac{1}{r} . \quad -(24)$$

These equations give:

$$\frac{d^2\phi}{dr^2} + \frac{1}{r}\frac{d\phi}{dr} - \frac{1}{r^2}\phi = -\frac{\rho}{\epsilon_0} . \quad -(25)$$

This equation was transformed into an undamped oscillator equation:

$$\frac{d^2\phi}{dR^2} + \kappa_0^2\phi = \exp\left(2i\kappa_0 R\right)\frac{\rho}{\epsilon_0} \quad -(26)$$

using the Euler transform {16}:

$$\kappa_0 r = \exp\left(i\kappa_0 R\right) . \quad -(27)$$

Eq. (26) was used to produce a Fourier analysis {1-11} for an assumed cosinal driving term (right hand side of Eq. (26)), and an equivalent circuit was designed. Resonant amplification of ϕ was shown to occur, and this phenomenon was studied in atomic hydrogen {1-11}. It was shown that the SCR mechanism can ionize the hydrogen atom and that the electron thus released could be used to produce electric power. In this section the driving term of Eq. (20) is used in Eq. (25) so that the overall process is shown to be the SCR amplification of the radiative correction.

If the Euler transform method is used, the mathematical problem to be solved is therefore as follows:

$$\frac{d^2\phi}{dR^2} + \kappa_0^2 \phi = \frac{\rho}{\epsilon_0} \cos\left(2\kappa_0 R\right), \quad -(28)$$

$$\rho = \frac{4\pi e}{\epsilon_0 \bar{V}_e} \cdot \left(\frac{\cos^2\left(\kappa_0 \left(R + R(vac)\right)\right)}{a_0^2 \kappa_0^2} \right) R^2(r), \quad -(29)$$

$$r + r(vac) = \frac{1}{\kappa_0^2} \cos\left(\kappa_0 \left(R + R(vac)\right)\right), \quad -(30)$$

$$\alpha = \langle \alpha \rangle \left(1 + \cos(\kappa r)\right). \quad -(31)$$

However, Eq. (25) can be solved directly by computer and this method is considered in a later article.

4. NUMERICAL DEVELOPMENT AND CIRCUIT DESIGNS (by Horst Eckardt)

5. OPTIMUM MATERIALS (by Gareth J. Evans)

4. NUMERICAL DEVELOPMENT AND CIRCUIT DESIGNS

In the following section we discuss results wich have been obtained by analytical and numerical studies. First we compare the description of the radiative corrections with the Spin Connection Resonance (SCR) mechanism derived in {17}.

4.1 Parameter studies

From Eqs.(9,11,12) the impact of the fine structure constant α on hydrogenic spectra can be described by the equation

$$-\frac{\hbar^2}{2m}\,\frac{\alpha}{2\pi}\,\frac{d^2P}{dr^2}+\left(V_{eff}^{(0)}-V_{eff}\right)=0 \qquad (32)$$

with

$$V_{eff}^{(0)}=-\frac{e^2}{4\pi\varepsilon_0 r}+\frac{l(l+1)\hbar^2}{2mr^2} \qquad (33)$$

and

$$V_{eff}=-\frac{e^2}{4\pi\varepsilon_0\left(r+r(vac)\right)}+\frac{l(l+1)\hbar^2}{2m\left(r+r(vac)\right)^2} \qquad (34)$$

If we describe this potential energy difference by a single SCR potential Φ, we have to replace

$$V_{eff}^{(0)}-V_{eff}\longrightarrow V_{SCR} \qquad (35)$$

and define

$$V_{SCR}=-e\phi \qquad (36)$$

The sign was chosen so that a positive contribution of the potential energy is obtained for high values of Φ. In this way we arrive at the expression

$$e\phi=\frac{e^2}{4\pi\varepsilon_0}\left(\frac{1}{r}-\frac{1}{r+r(vac)}\right)-\frac{l(l+1)\hbar^2}{2m}\left(\frac{1}{r^2}-\frac{1}{\left(r+r(vac)\right)^2}\right) \qquad (37)$$

That this expression makes sense can be seen from considering the limits of vanishing or infiite vacuum interaction, expressed by r(vac):

$$r(vac) \to 0 \quad \Rightarrow \quad e\phi \to 0 \qquad (38a)$$

$$r(vac) \to \infty \quad \Rightarrow \quad e\phi \to -V_{eff}^{(0)} \qquad (38b)$$

In the maximum case the SCR potential cancels out the atomic effective potential energy so that Eq. (10) becomes identiacal to that of a free particle. In general Φ is orbital dependent as was also found in {17} by numerical studies.

In Eq.(37) we have three parameters being of principal interest: Φ, r, and r(vac). In the first three Figures we present the dependence of Φ on r(vac) for fixed r values. Near to the atomic core (Fig. 1, r=0.1; all quantitites given in atomic units) only the s orbitals (l=0) lead to a positive SRC potential, for other orbitals the interaction gives a decrease in potential energy which counteracts a resonance effect. From our earlier studies {18} we know that the vacuum interaction is much smaller then so that a positive SCR effect results. The same holds for a radius in the valence region (r=1, Fig. 2). In the outer atomic region (r=5, Fig. 3) all contributions become positive, but small. A surface plot Φ(r(vac), r) for angular momentum quantum number l=0 is presented in Fig. 4. Positive values of Φ are generally obtained for small radii r.

The Figures 5-7 show the dependence of r(vac) from Φ, again for three fixed radii r. There is a pole in r(vac) which moves in direction of Φ=0 for increasing r. Left-hand of the pole we have positive r(vac) values for l=0 which show some kind of resonance enhancement when approaching the pole. From the surface plot (Fig. 8) we see that such an enhancement only takes place in a small band of the r-Φ plane.

4.2 Oscillatory r(vac)

The results so far were obtained for a non-oscillatory r(vac). Next we use the oscillatory model (3) of the fine structure constant. According to Eq.(12) we have to solve

$$\frac{d^2P}{dr^2} = \frac{4\pi m}{\hbar^2 \alpha}\left(V_{eff}^{(0)} - V_{eff}\right)P \qquad (39)$$

for the variable r(vac). Using computer algebra {19} this gives a complicated rational function of order 3 in r. In (39) we replace furthermore

$$\alpha = \langle\alpha\rangle\left(1 + \cos(kr)\right) \qquad (40)$$

with

$$\langle\alpha\rangle = 0.007297 \qquad (41)$$

obtaining a solution of (39) which is dependent on a wave number κ. For P(r) we choose the undisturbed radial functions of the Hydrogen atom. Since P(r) depends on the quantum number l, this dependence propagates into the solution of (39). The result for three l values is

graphed in Fig. 9. r(vac) for the 1s orbital strongly oscillates for large radii, but this is in a region where the probability density is very small.

Having obtained the function r(vac) (κ, r), we can proceed now with solving the resonace equation (25). This equation has been transformed into an oscillator equation without damping (26) as was originally described in {17}. The radial coordinate r has been transformed to another coordinate R as given by (27). Therefore we must transform the function r(vac)(r) to r(vac)(R) to be able to use it for the driving charge density ρ(R) at the right-hand side. Unfortunately Eq.(27) is periodic in R and restricted in range. We can construct a bijective mapping for the whole r range by taking the real part of (27) in the form

$$K_0 r = \cos\left(\kappa_0 R \pm 2\pi n\right) \qquad (42)$$

with an integer n. The inverse transformation then is

$$R = \frac{1}{\kappa_0}\left(\arccos\left(\kappa_0 r\right) \pm 2\pi n\right) \qquad (43)$$

We use this equation to calculate the requested function r(vac)(R). Choosing n in a suitable way, we obtain the behaviour as shown in Fig. 10 where R is continuously defined over the full range of r. The oscillation of α leads to the behaviour shown in Fig. 11 for r(vac) of the 2s orbital. The nonlinear transformation (43) infers the crookbacked form.

4.3 Resonance

Now we have all elements available to set up Equ.(28) and to construct a numerical solution. By means of Eqs.(19,20) we have

$$\rho(r) = A\,(r + r(vac))^2\, R_\ell^2(r) \qquad (44)$$

with a normalization factor A which is computed numerically; $R_l(r)$ is the radial wave function of Hydrogen. We transform ρ(r) to ρ(R) by defining a uniform R grid and back-transforming it to an r grid according to (42). Since ρ(r) is given analytically, we can evaluate it on the non-uniform r grid without problems. We can solve now

$$\frac{d^2\phi}{dR^2} + \kappa_0\phi = f(R) \qquad (45)$$

with

$$f(R) = \frac{\rho(R)}{\varepsilon_0}\cos\left(2\kappa_0 R\right) \qquad (46)$$

In order to obtained resonances in the solution, we had to make two modifications: The relative strength of r(vac) in Eq. (44) had to be enhanced by a factor of 1000 and the driving force (46) had to be enhanced by the same factor as well. While the latter is an uncritical operation due to the unspecified normalization factor in (44), The enhancement of r(vac) can be made plausible by the following: This calculation is restricted to a single atom where ρ(R) is constrained to a few Bohr radii. In an atomic lattice of a solid, the excitation goes over many atoms where resonance can enhance this in a nearly unbound spatial region. Therefore it

may be justified to enlarge r(vac) in this model calculation. As an additional approximation we identify the two wave numbers κ and κ_0 in Eqs. (40) and (46) as we did in earlier SCR calculations {17}.

The driving charge density thus enhanced is graphed in Fig. 12. The two maxima of the atomic 2s distribution are still visible, strongly superimposed with oscillations. The total driving force is shown in Fig. 13. The zero at R=3 is propagated from the zero in Fig. 12. Finally we present the numerical solution $\Phi(R)$ in Fig. 14. One can see that there is a resonance for the second wave number κ=5. Since f(R) is restricted in space, the resonance does not grow further outside the "definition volume". This behaviour reflects the above discussion about the restrictions of the model.

The resonance behaviour is clearly seen from the resonance diagram, Fig. 15. The maximum of the amplitude taken over 15 wave lengths is plotted. The main peak is at half the frequency of a pure cosine driving force $\cos(\kappa_0 r)$, and there are several secondary maxima visible. The structure is somewhat richer than for the earlier SCR calculation {17}, but has the feature of the halved resonance frequency in common with it.

4.4 Relation to Circuits and SCR applications

To some it may seem that Spin Connection Resonance (SCR - as developed in this series of papers) suggests that a vast and renewable source of energy is available from nowhere violating the conservation of energy and momentum, but this is not the case. Spin Connection Resonance is a resonance of General Relativity that fully conserves energy momentum as rigorously established in this series of papers. The overall mechanism is one in which the well known radiative correction (Lamb 1946, Bethe 1947) is amplified by Spin Connection Resonance. The resonances are caused by amplification of the ubiquitous electric and magnetic fields that are responsible for the well observed radiative correction. The amplification is controlled by an undamped resonance equation. The driving term comes from a solution of the Schrodinger equation with radiative correction. The resonance equation can be used to design a circuit.

The resonance equation (45/46) can technically be realized by an equivalent circuit as already described in detail in {17}. The driving force has to be provided electrically. This force is characterized by its Fourier spectrum. However, we do not have a continuously periodic function as in {17} since one single atom which is considered in our model is not a periodic structure. Therefore we choose the usual proceeding in such cases: we cut the function f(R) at an appropriate radius (here R=15) and assume periodicity with a wavelength of λ=15. For each given κ we obtain separate functions $f(R, \kappa)$, and consequently different Fourier spectra for each κ value. These are shown in Fig. 16 for the three κ values investigated. The structures are similar but shifted in frequency. This means that there is a common pattern in the structure of the driving force. This could be like a "fingerprint" for a certain atomic structure.

Another type of SCR devices are the various types of Bedini motors, or more precisely, motor-generators {20}. According to the block diagram of Fig. 17, they consist of a motor part, a generator part, and a control circuit. The generator part which takes up the potential from spacetime is a series resonance circuit as can be seen from the diagram. The motor and the control part are there to generate a suitable form of the driving force and are coupled inductively. We must restrict comparison to this logical level. It should become clear that the functioning of the Bedini motor-generator is based on the principle that we have derived from the equivalent circuit. A more direct application of the mechanisms can take place in solid state chemistry as is discussed in the next section.

It has been suggested {21} that the Bedini - Cole device seems to meet the basic requirements of a SCR design that can be used for Space Energy utilization. The "driving force" in this device is a voltage spike produced by a collapsing magnetic field on a coil. A well defined resonance condition is generated by the voltage spike. An ionic electrolyte solution of a storage battery is used as the source of electrons (and not a metal as suggested below). Details of this device need to be investigated further within the ECE framework developed in this paper.

5. DISCUSSION OF MATERIALS BEING SUITED FOR SCR

There are a number of claims in the literature, dating back to Tesla at the end of the twentieth century (more recently developed by Horta) that seem to support the principle of Spin Connection Resonance (and the availability of Space Energy). The reports of resonances that led to paper 63 in this current series were based on the resonance work of Tesla. Bedini has reported the development of devices that may be utlising Space Energy and Grabiel's Kron's work on motors is another interesting line of interesting research in this context. Kron's electrical circuits seem to offer the prospect of working backwards from a well designed engineers' circuit to SCR equations.

When a working circuit is available it can be analysed with ECE theory to find its equivalent resonance equation, spin connection and driving term. The latter is traced back to jitterbugging of the electron in an orbital (the radiative correction of Lamb and Bethe).

The alternative approach is to develop new circuits from SCR equations of various kinds and develop working devices from first theoretical principles. Circuit diagrams can in principle be constructed for different types of driving forces and then compared, where available and appropriate, with circuits of reported working devices (to optimise and "fine tune" them).

Numerical solutions for the Euler transformed resonance equation discussed above indicate that resonances are obtained but only over many atoms in a solid. The solutions also suggest that not every possible form of oscillating driving force gives a resonance. This needs to be developed and better understood. The solutions suggest that metals with s valence states may be particularly suited for SCR. They show that the radiative correction can be amplified to ionise the s electron of valence one metals, for example, or Any compound in which there is an ns valence electron loosely bound to the nucleus (that can be "easily" ionised into a free electron to produce an electric current).

This suggests that attention should be focused, in these early stages of development, on materials with low Work Functions (ϕ) in the solid state for their potential use in designing new circuits. Density functional code could be used to produce the work function of solids from quantum mechanics. The effect of the amplified Lamb shift could then be computed to see the effect on the material with the lowest work function. The important point is that the driving force can initially be very small (the radiative correction is very small) but can be amplified by an Euler Bernoulli resonance equation. The Lamb shift is in effect the driving force and resonant amplification of the radiative correction occurs through the spin connection of unified field theory as discussed above.

5.1 Materials that could be considered in device development

The well known work function (ϕ) is the measure of the energy required to extract an electron from a solid – from the highest filled level in the Fermi distribution of a solid.

Thermionic

Richardson's equation gives an estimate of the work function:

(47) $I = AT^2 \exp(-\Phi/kT)$

where I is the thermionic current, T the absolute temperature, k is Boltzmann's constant and A is a constant (having a theoretical value 120 amp cm^{-2} deg^{-2}).

Photoelectric

The Work Function can be estimated photoelectrically for metals. Einstein's expression for the photoelectric effect is $h\nu = e\Phi + E$, where E is the kinetic energy of the ejected photoelectron. The photoelectric current J released when light of energy $h\nu$ falls on the surface of a metal, for which the threshold frequency is given by $h\nu_0 = e\Phi$ (for then $E = 0$), is given by the Fowler equation

(48) $J = B(kT^2).f\{(h\nu - h\nu_0)/kT\}$

where f is a universal function of (hv − hv0)/kT and B is constant provided that $h\nu$ is near to $h\nu_0$.

Contact Potential difference (CPD)

The Work Function can also be estimated by the contact potential difference (c.p.d.) VAB that exists between the surfaces of two solids A and B of work functions Φ_A and Φ_B, when connected electrically, since

(49) $\Phi_B - \Phi_A = eV_{AB}$

for the two solids at the same temperature. The method involves a prior knowledge of the work function of one of the solids if that of the other is to be measured absolutely.

Electric Field Emission

A fourth method involves the field emission of electrons when an external electric field F is applied.

Adsorbates or contaminants will usually reduce the measured Φ and different crystal faces of the same material may have different values of Φ. "Doping" also reduces the work functions of metals. A table of Work Functions for metals is reproduced below (taken from {22}).

Table 1. Work functions of metals.

Metal	**Work function φ/eV**		**Metal**	**Work function φ/eV**		
	Photoelectric	**C.P.D.**		**Thermionic**	**Photoelectric**	**C.P.D.**
Li . . .	—	2.32	Nb . . .	4.30	—	4.37
Na . . .	2.36	2.46	Mo . . .	4.33	4.49	4.21
K . . .	2.30	2.01	Ta . . .	4.33	4.30	4.22
Rb . . .	2.05	—	W . . .	4.55	4.55	4.55
Cs . . .	1.95	1.82	Re . . .	4.72	—	—
Be . . .	—	3.91	Ti . . .	4.10	4.33	4.20
Mg . . .	—	3.61	Cr . . .	4.60	4.44	—

Ca . . .	2.87	—	Mn . . .	—	4.08	—
Ba . . .	2.52	2.35	Fe . . .	—	4.60	4.16
			Co . . .	—	4.97	—
Zn . . .	3.63	4.11	Ni . . .	5.24	5.15	5.25
Cd . . .	—	4.22				
			Zr . . .	4.00	—	—
Al . . .	4.28	4.19	Hf . . .	3.65	—	—
Ga . . .	4.35	—				
In . . .	4.08	—	Ru . . .	—	4.71	4.73
			Rh . . .	4.72	—	—
Sn . . .	4.28	4.43	Pd . . .	—	5.40	—
Pb . . .	4.25	3.83	Ir . . .	4.57	—	—
			Pt . . .	5.36	5.63	—
Cu . . .	4.65	4.51				
Ag . . .	4.26	4.29	Th . . .	—	—	3.71
Au . . .	5.10	5.28	U . . .	3.47	3.47	3.63
As . . .	4.79	—	C (dag) . .	—	—	4.65–5.0
Sb . . .	4.56	—	Si . . .	—	4.95	4.75
Bi . . .	4.34	—	Ge . . .	—	5.15	4.83

It can be seen that the metal Caesium has the lowest work function. If we consider this metal as an example for potential use in the design of a SCR circuit, there are two well documented resonance effects in this metal:

a) Photoelectric Effect

As a photosensitor, Caesium has a peak response at 800nm in the infrared, both thermal and photoemission of electrons is very high because of the low work function. Caesium is a very reactive metal and is only naturally occurring in relatively small amounts. Alloys of Caesium (with antimony, gallium, indium, and thorium for example) are all generally photosernsitive and may be more stable and useful for device experimentation.

b) Caesium Ion Resonance

Caesium is also used as an atomic clock, a standard measure of time, based on the caesium ion resonance of 9,192,631,770Hz.

It would be interesting to try to reproduce these resonances with density functional code and to amplify them with a circuit based on the resonance equations developed in this paper.

Other lessreactive and more stable metals and materials with low work functions also need to be investigated. Diamond, for example, is one of the few materials with a known negative work function.

5.2 Small Initial Driving Forces

The driving forces used to stimulate resonances could be electric, magnetic, electromagnetic or a combination of two or all three but numerical solutions of the equations seem to suggest that not every possible form of oscillating driving force gives a resonance and this needs to be fully understood and developed. To reiterate, the initial driving force can may be very small (the radiative correction is very small) but this can be amplified by an Euler Bernoulli resonance equation.

It is well known that metals CAN be stimulated with electromagnetic fields to release electrons - the photoelectric effect. It is also well known that electric fields can be used to stimulate metals to release electrons - Field Emission. Using a magnetic field (or a combination of fields) as a small initial "driving force" to release electrons is interesting. In general all emissions can be enhanced by finely tuning a circuit designed from the SCR equations developed in this paper.

In concluding, we set out in this paper the factors that emerge from the ECE theoretical framework that control the development of SCR devices. The theory and its solutions is available as a guide for designing new devices and for working backwards from any existing device to optimize and fine tune its performance. The theory can be used as a guide for the types of material that may be of interest (doped materials, semi conductors, and superconductors, as well as nS valence metals, spring to mind). We should be thinking in terms of circuits developed from the Euler equations and then experimenting with different driving forces. When we have an appropriate circuit and material we need to experiment to find and optimize a resonance (a spike of voltage from a small input) and use ECE theory to fully understand and develop what is taking place.

In summary:

1) Resonances – arise from amplification of magnetic and electric fields that are responsible for the radiative correction.
2) Amplification – is controlled by an undamped resonance equation.
3) Driving Term – comes from a solution of the Schrödinger equation with radiative correction.
4) Circuits – can be designed from the resonance equation.
5) Optimum Materials – seem to be solids that ionize readily (but semiconductor and superconducting materials also spring to mind).

ACKNOWLEDGMENTS

The British Government is thanked for a Civil List Pension to MWE for distinguished contributions to science, and the staff of AIAS and many others are thanked for invaluable voluntary work and many interesting discussions.

REFERENCES

{1} M. W. Evans, "Generally Covariant Unified Field Theory" (Abramis Academic, Suffolk, 2005), vol. 1.

{2} M. W. Evans, ibid., Volumes 2 and 3 (2006).

{3} M. W. Evans, ibid., vols. 4 and 5 in prep. (Papers 55 to 87 on www.aias.us).

{4} L. Felker, "The Evans Equations of Unified Field Theory" (Abramis Academic, Suffolk, 2007, in press); A. D. DeBruhl, "The Ultimate Truth" (Published Oct 2006, amazon).

{5} H. Eckardt, L. Felker, D. Indranu, S. Crothers, K. Pendergast and G. J. Evans, contributions on www.aias.us.

{6} M. W. Evans, precursor gauge theories to ECE, Omnia Opera Section of www.aias.us, 1992 to present.

{7} M. W. Evans and L. B. Crowell, "Classical and Quantum Electrodynamics and the B(3) Field" (World Scientific, 2001).

{8} M. W. Evans, ed., "Non-Linear Optics", a special topical issue in three parts of I Prigogine and S. A. Rice (series editors), "Advances in Chemical Physics" (Wiley, New York, 2001, second edition hardback and e book), vols. 119(1) to 119(3), endorsed by the Royal Swedish Academy; ibid., M. W. Evans and S. Kielich (eds.), first edition, (Wiley, New York, 1992, 1993 and 1997 (softback)), vols. 85(1) to 85(3), prize for excellence, Polish Government.

{9} M. W. Evans and J.-P. Vigier, "The Enigmatic Photon" (Kluwer, Dordrecht, 1994 to

2002, hardback and softback) in five volumes.

{10} M. W. Evans and A. A. Hasanein, "The Photomagneton in Quantum field Theory" (World Scientific, 1994).

{11} M. W. Evans, Acta Physica Polonica, 38, 2211 (2007).

{12} S. P. Carroll, "Space-time and Geometry: an Introduction to General Relativity" (Addison Wesley, New York, 2004, also available on web), chapter three. See also the papers by D. Indranu on www.aias.us on advanced Cartan geometry.

{13} S. Weinberg, "The Quantum Theory of Fields" (Cambridge Univ. Press, 2005, softback).

{14} L. H Ryder, "Quantum Field Theory" (Cambridge Univ. Press, 1996, softback).

{15} P. W. Atkins, "Molecular Quantum Mechanics" (Oxford Univ. Press, 1983, 2nd. Ed., and many subsequent editions in softback).

{16} G. Stephenson, "Mathematical Methods for Science Students" (Longmans, London, 1968, fifth impression softback and subsequent impressions).

{17} M. W. Evans, "Generally Covariant Unified Field Theory" (Abramis 2007 / 2008), vol.4, chapter 7, "Space-time Resonance in the Coulomb Law".

{18} Papers 85 and 86 of the ECE series, www.aias.us and www.atomicprecision.com.

{19} Maxima computer algebra system, http://maxima.sourceforge.net/.

{20} "All About Tesla", a film directed by Michael Krauss which premiered in Berlin in May 2007 and has been shown in the Cannes Film Festival and Dylan Thomas Centre in Swansea, general release.

{21} John Shelburne, communication 2007.

{22} G. P. Owen, communication 2007.

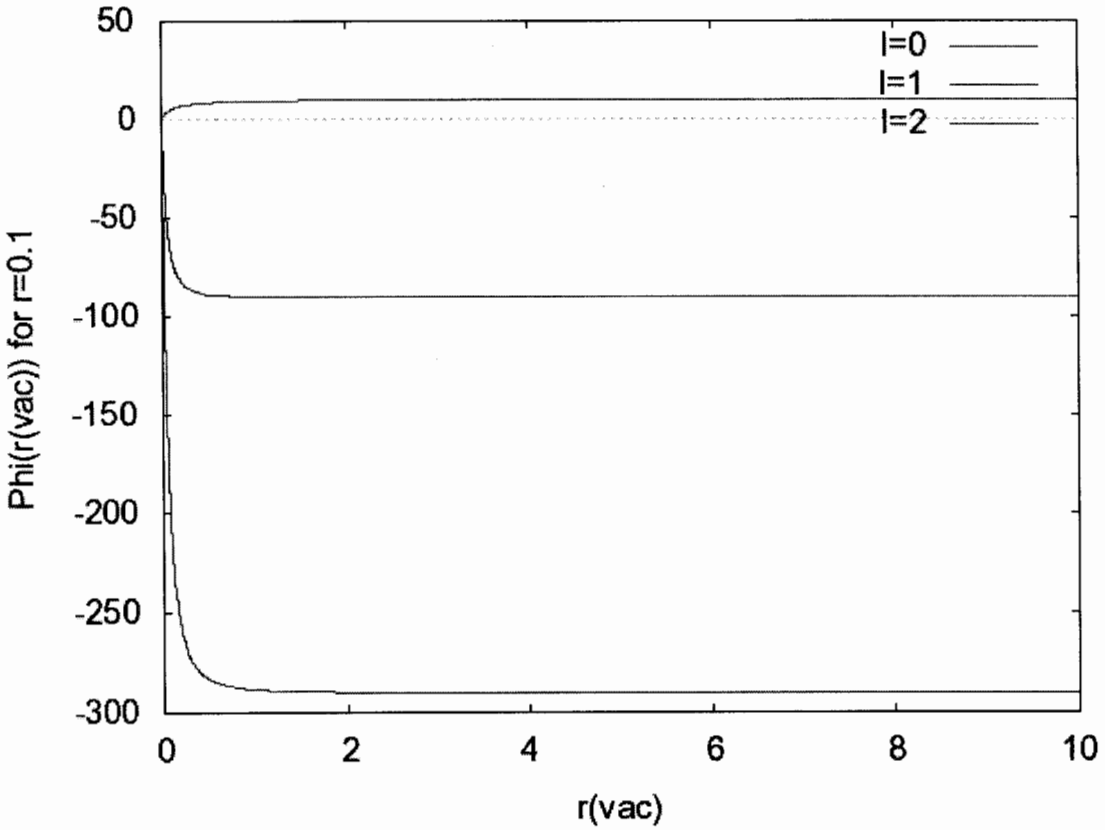

Fig. 1. Φ(r(vac)) for fixed r=0.1.

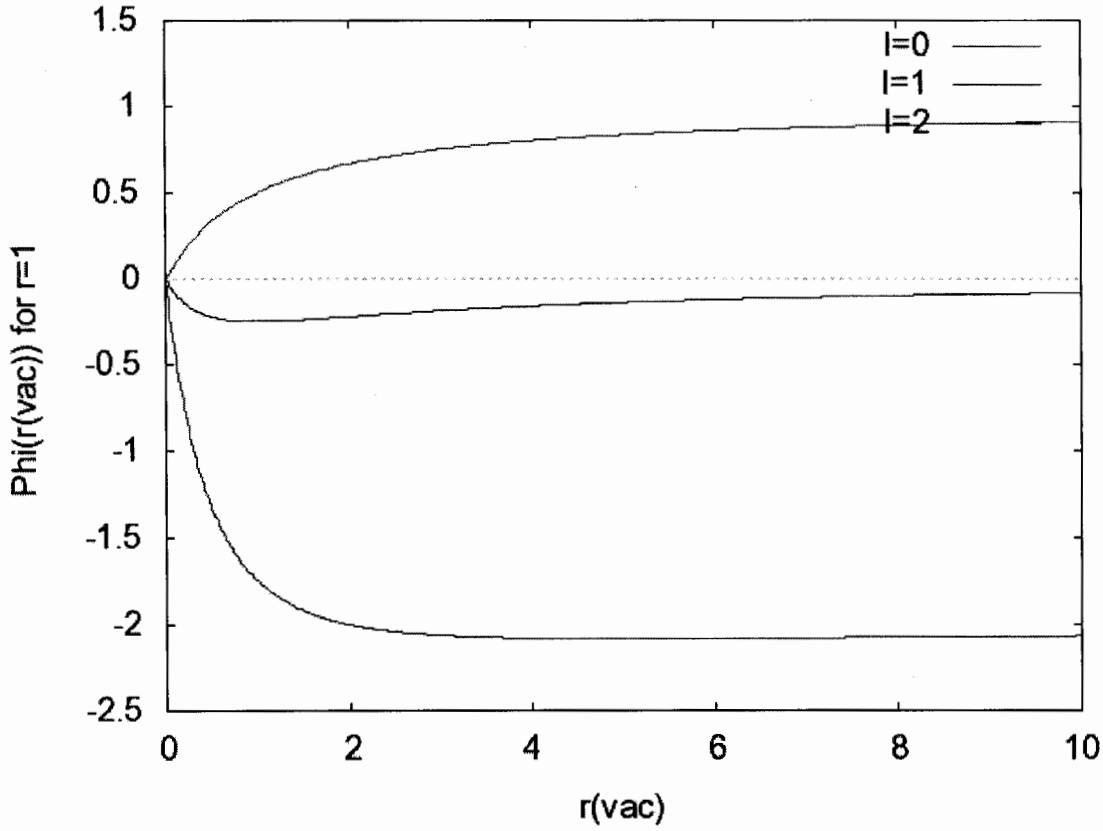

Fig. 2. Φ(r(vac)) for fixed r=1.

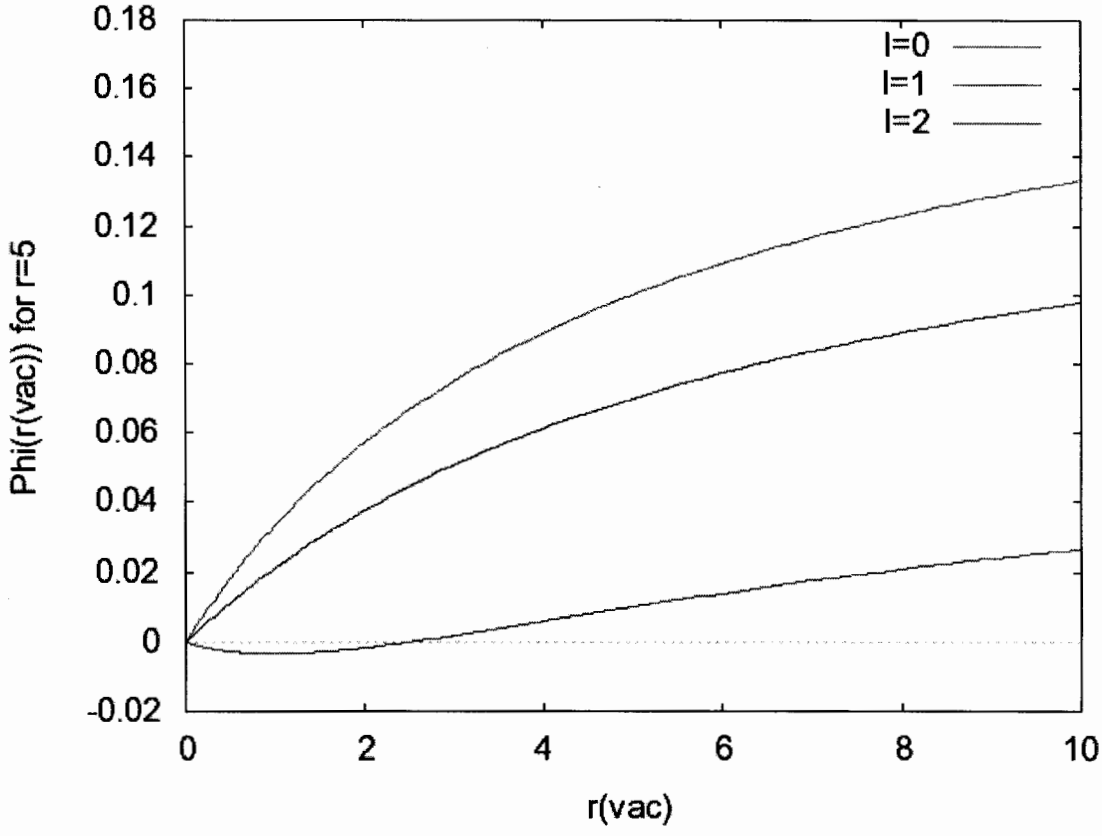

Fig. 3. Φ(r(vac)) for fixed r=5.

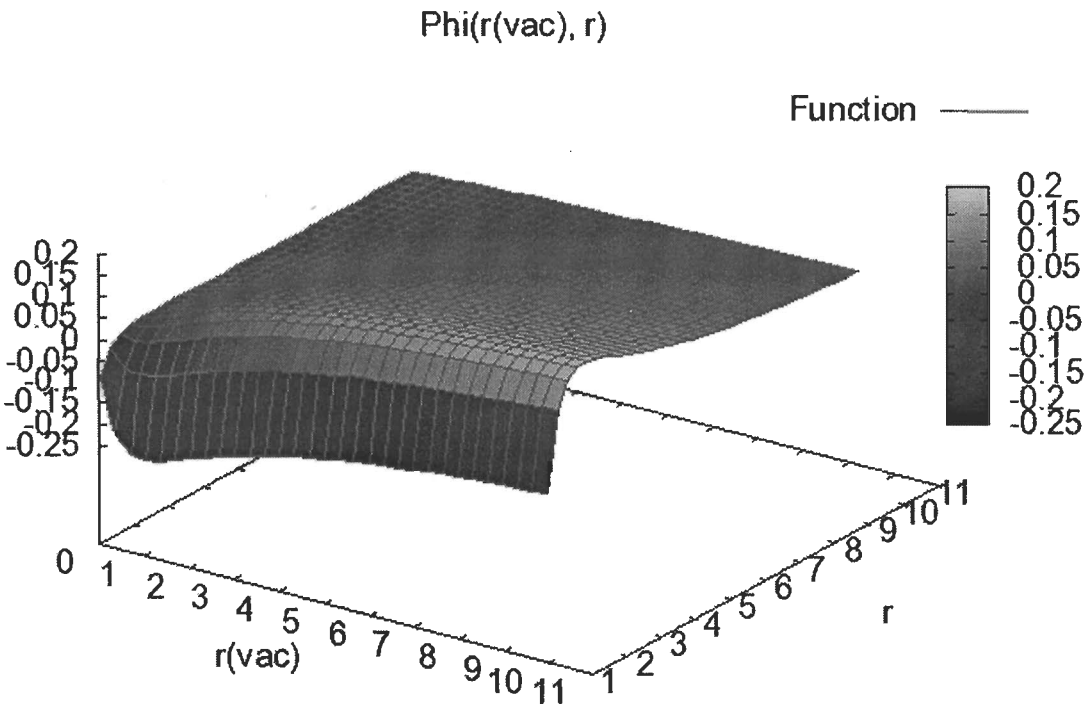

Fig. 4. Surface plot Φ(r(vac), r) for angular momentum quantum number l=0.

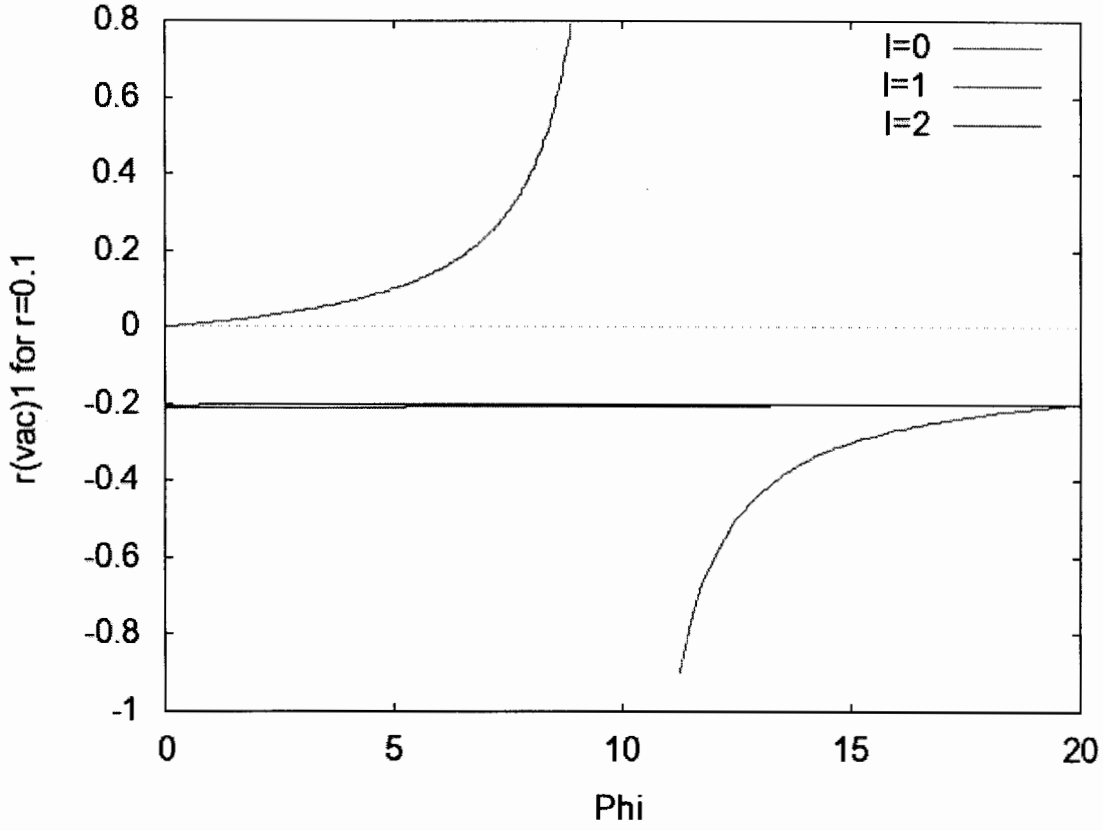

Fig. 5. r(vac) (Φ) for fixed r=0.1.

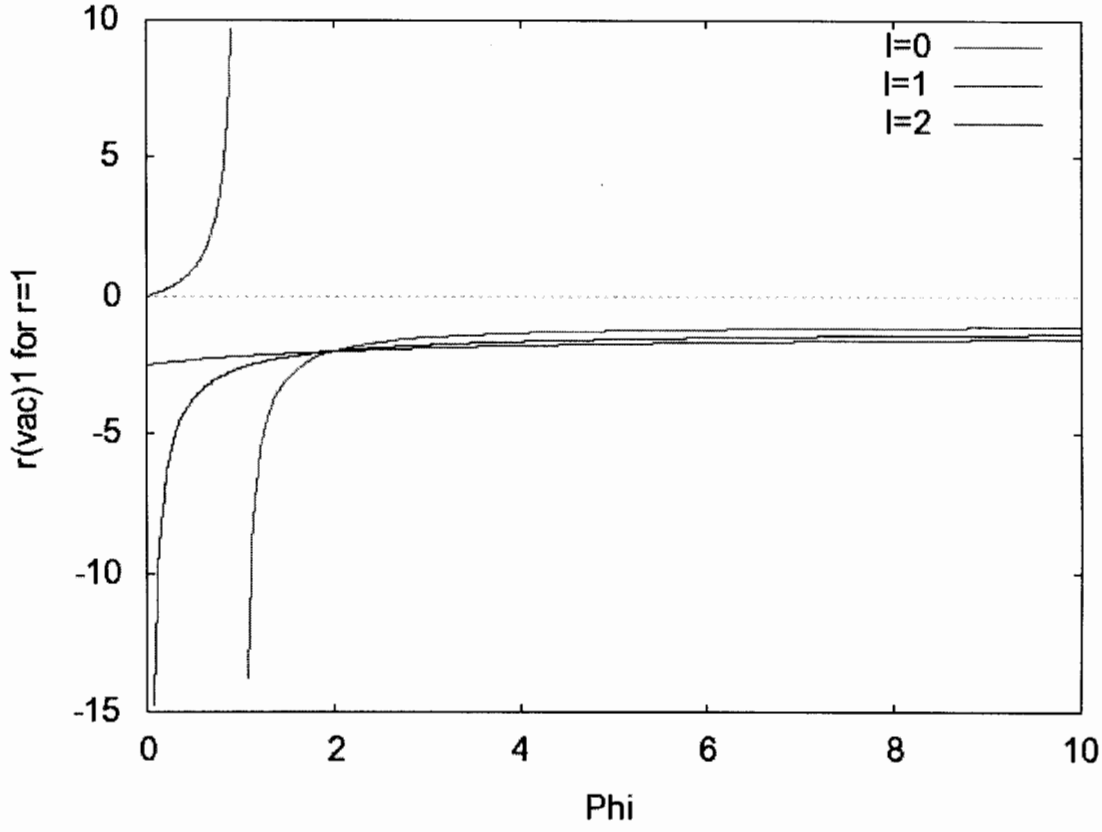

Fig. 6. r(vac) (Φ) for fixed r=1.

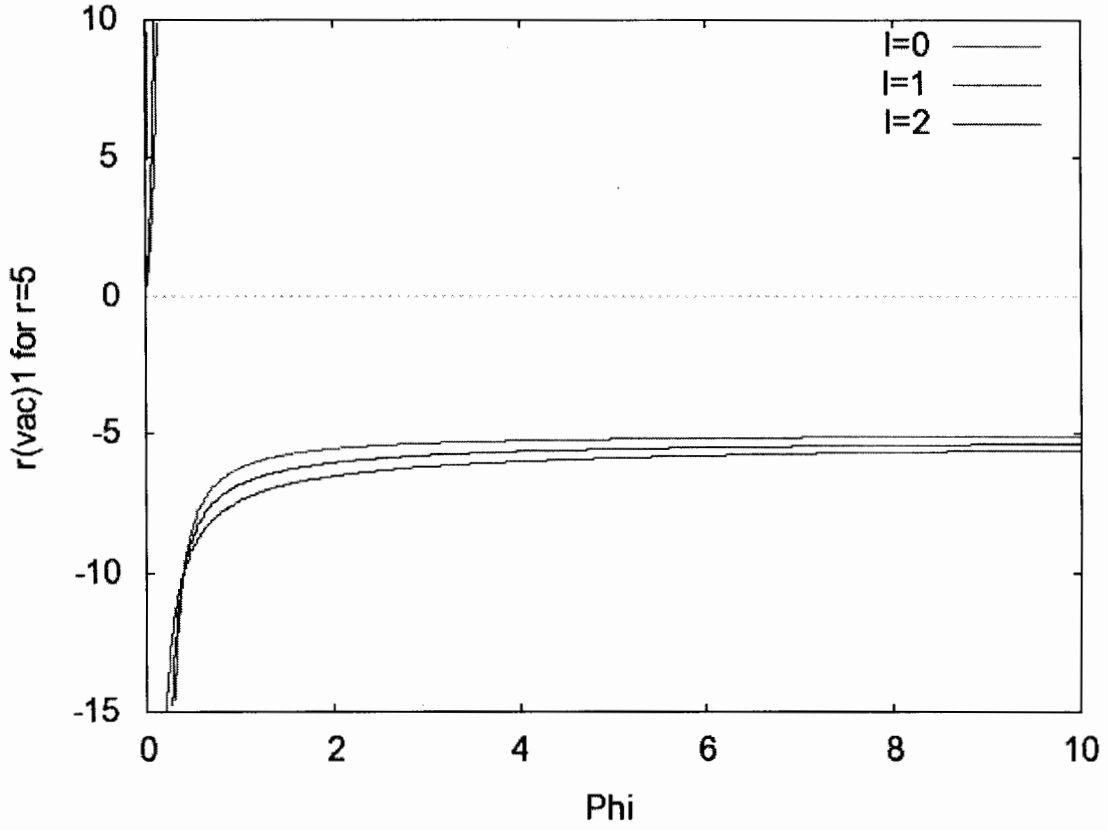

Fig. 7. r(vac) (Φ) for fixed r=5.

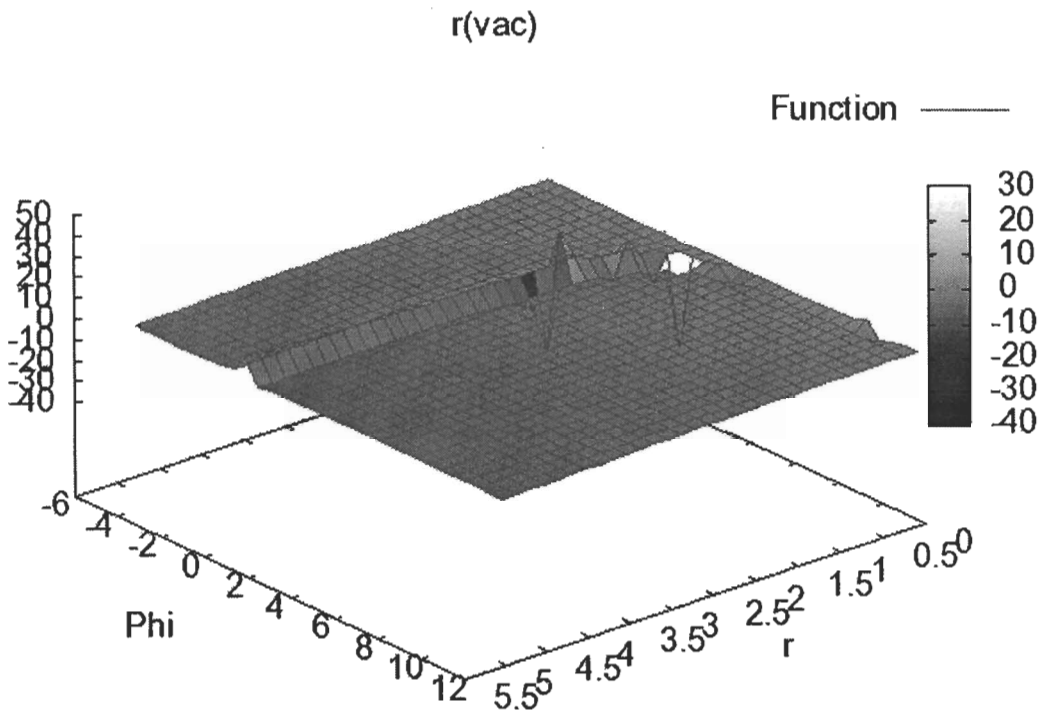

Fig. 8. Surface plot r(vac) (Φ, r) for angular momentum quantum number l=0.

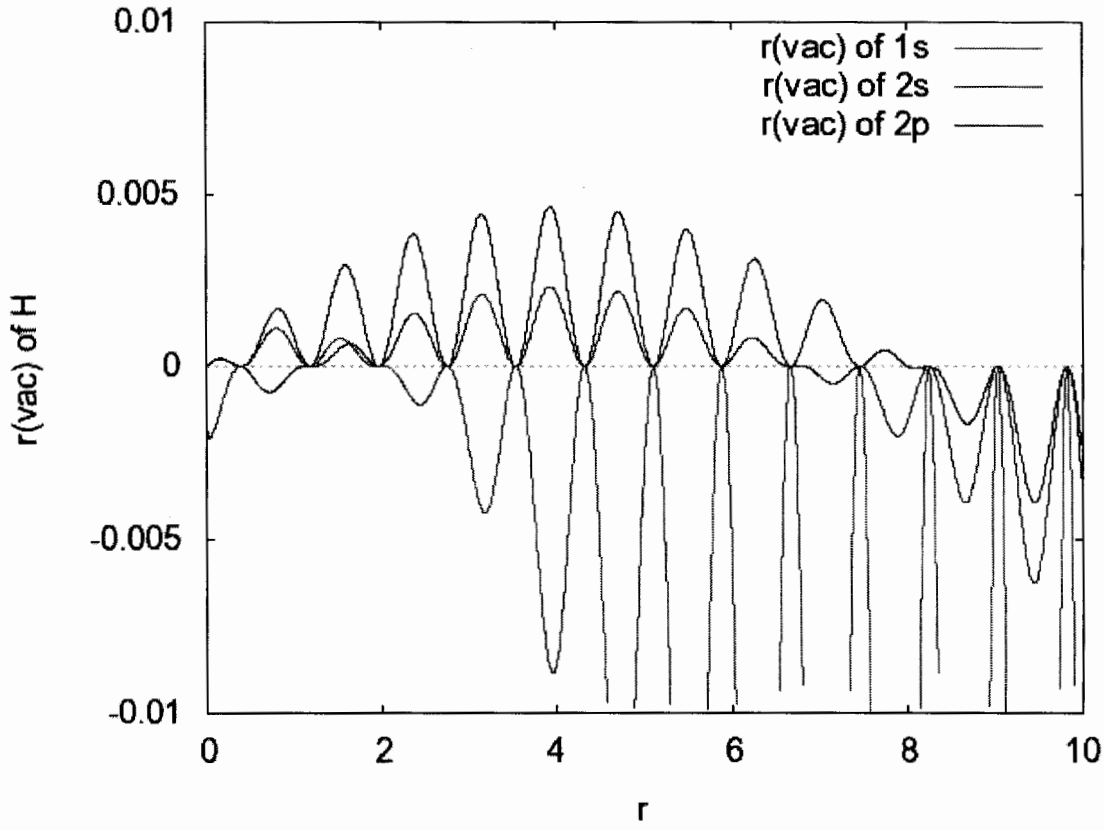

Fig. 9. Oscillating r(vac) for three orbitals of H for κ=8.

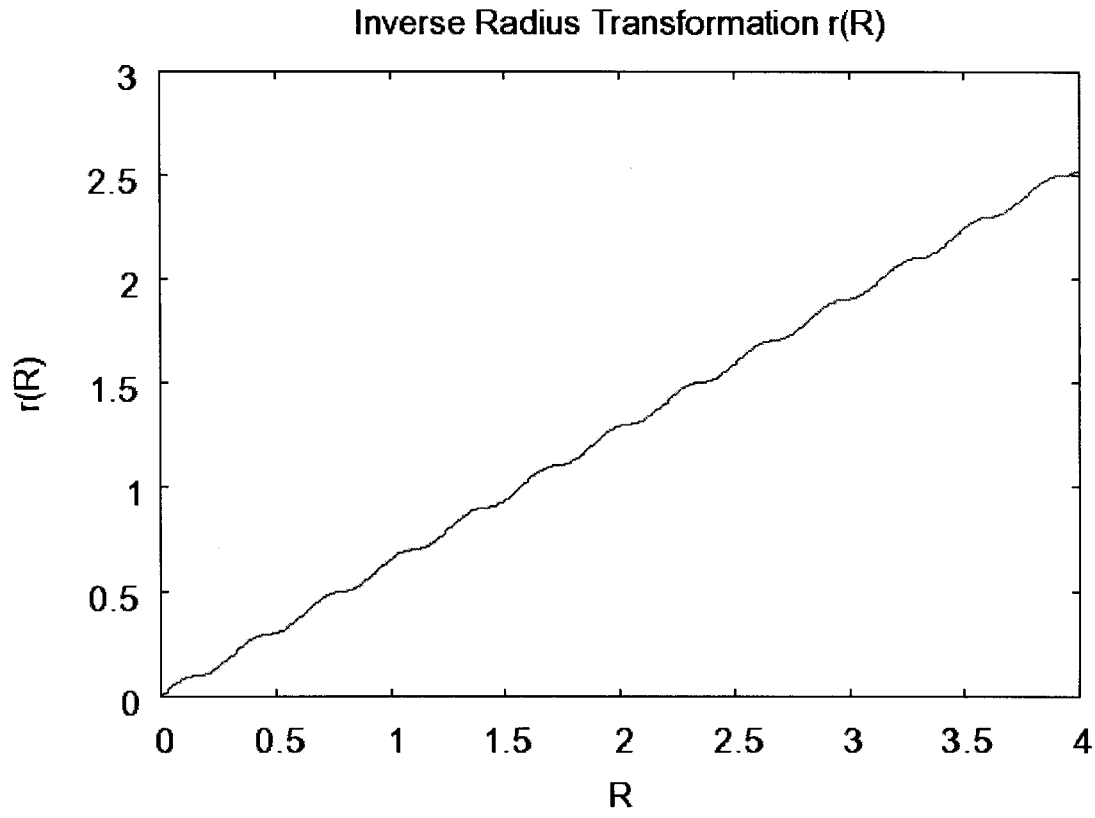

Fig. 10. Radius back transformation r(R).

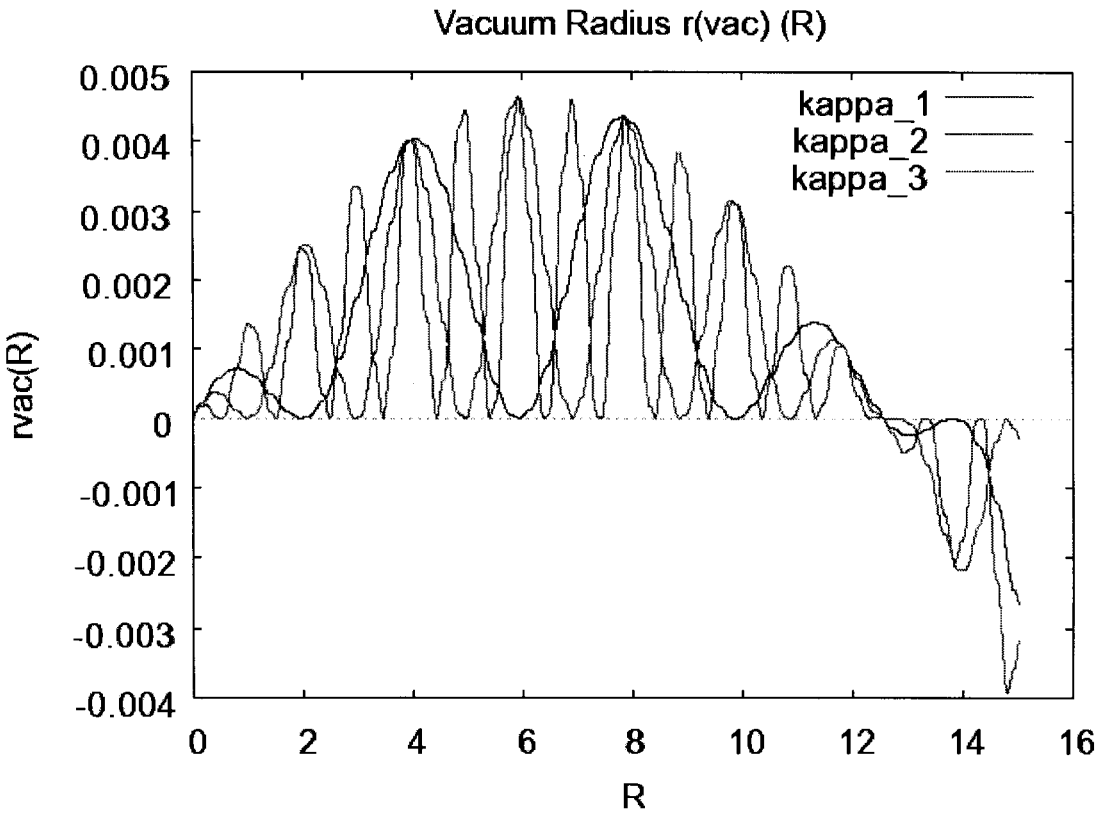

Fig. 11. Oscillating vacuum radius r(vac) (R) of the 2s orbital for three wave numbers (2.5, 5, 10).

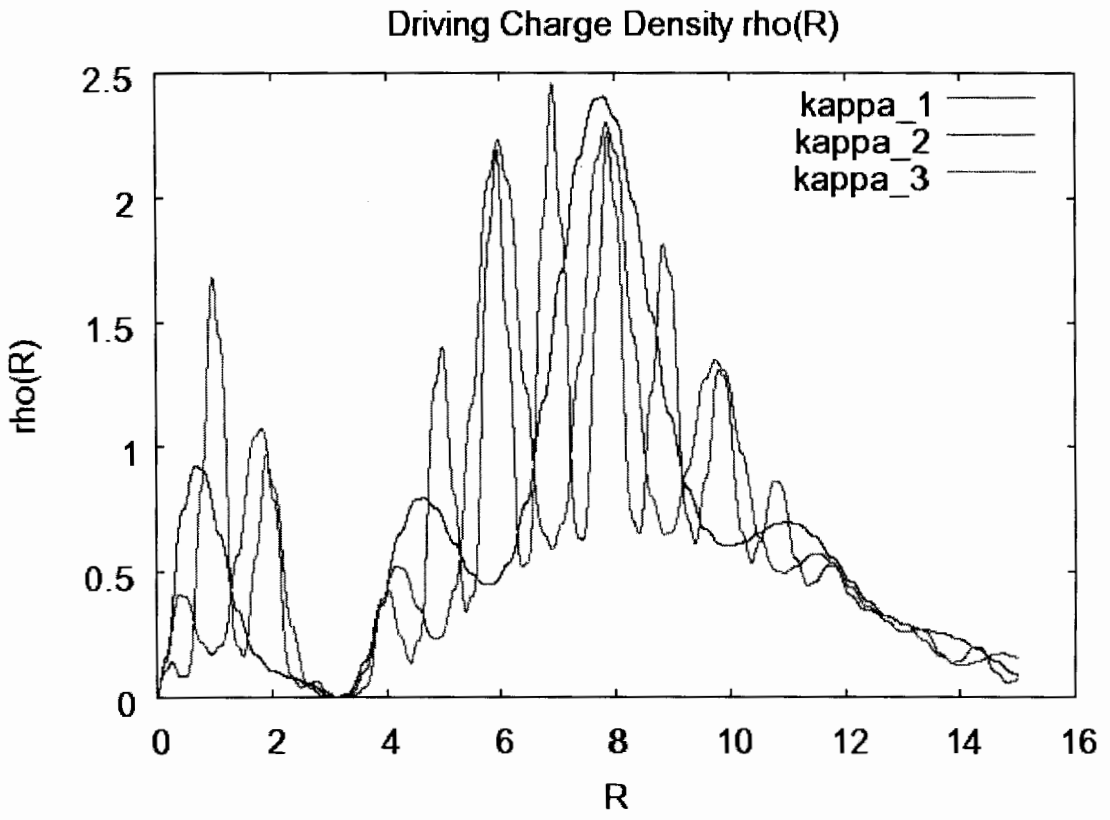

Fig. 12. charge density of driving charge density ρ(R) equation for three wave numbers (2.5, 5, 10).

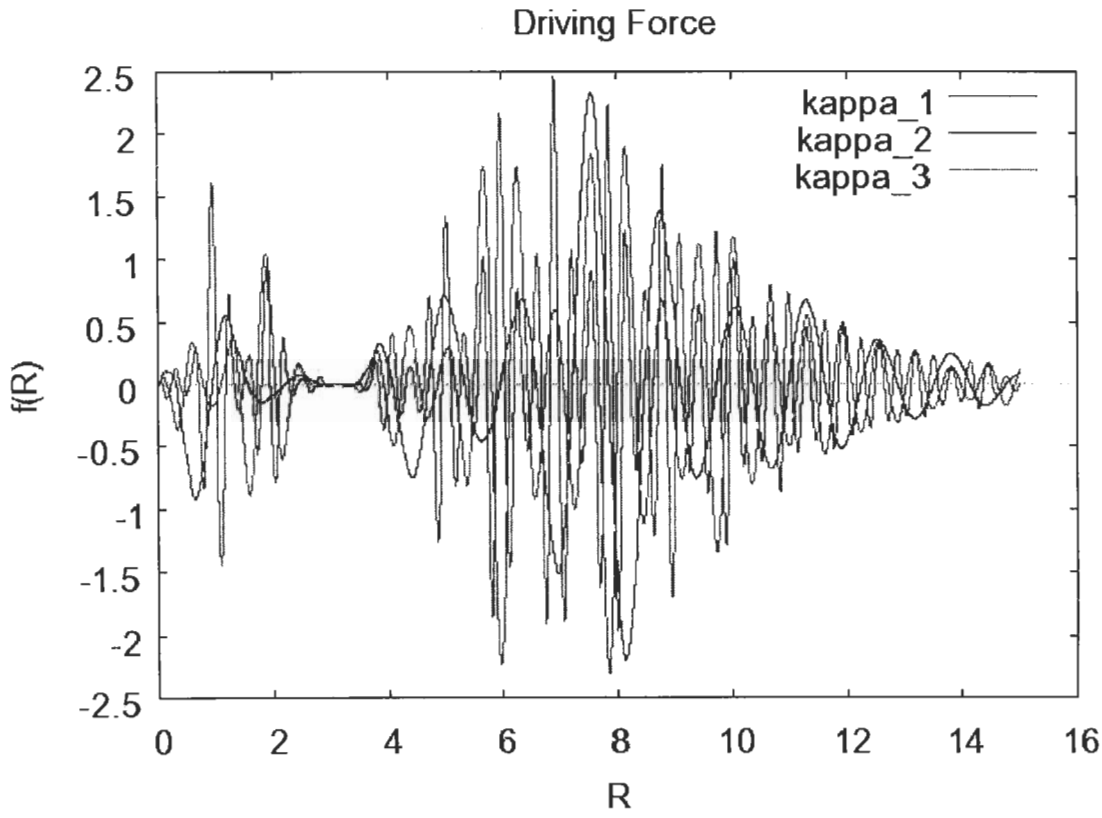

Fig. 13. Driving force f(R) for for three wave numbers (2.5, 5, 10).

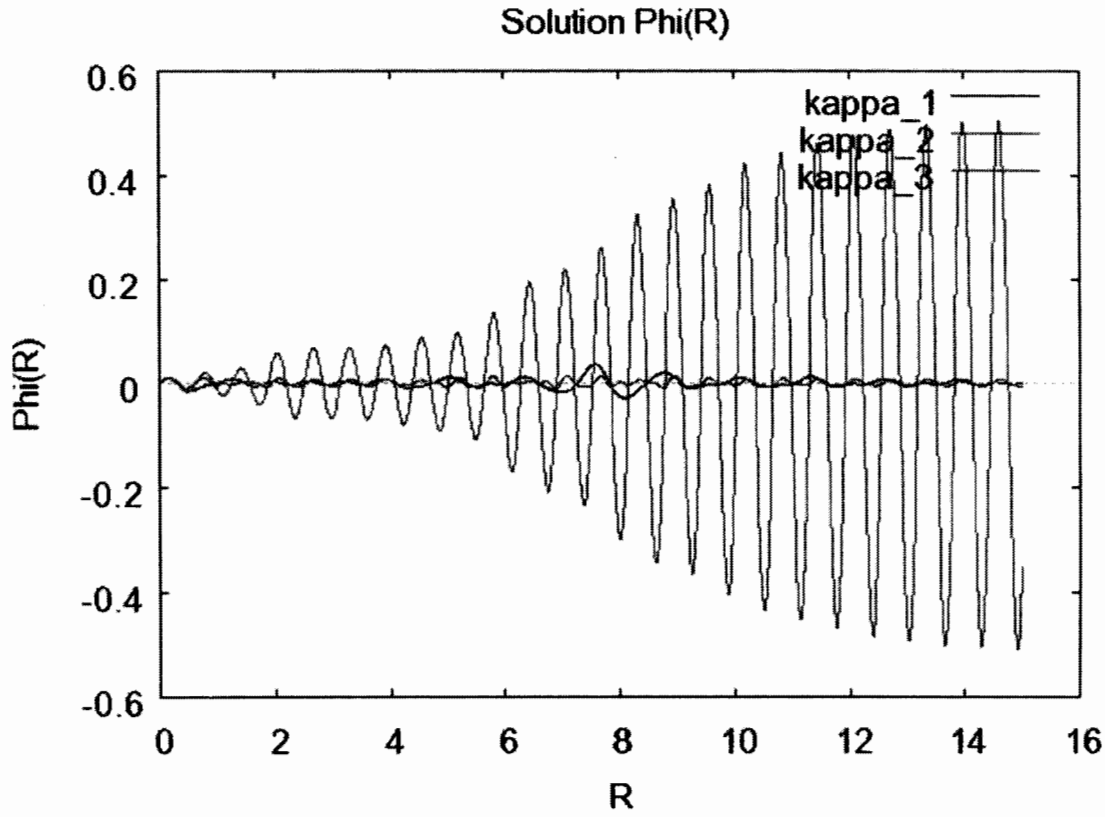

Fig. 14. Solution of $\Phi(R)$ of Euler transformed equation for three wave numbers for three wave numbers (2.5, 5, 10).

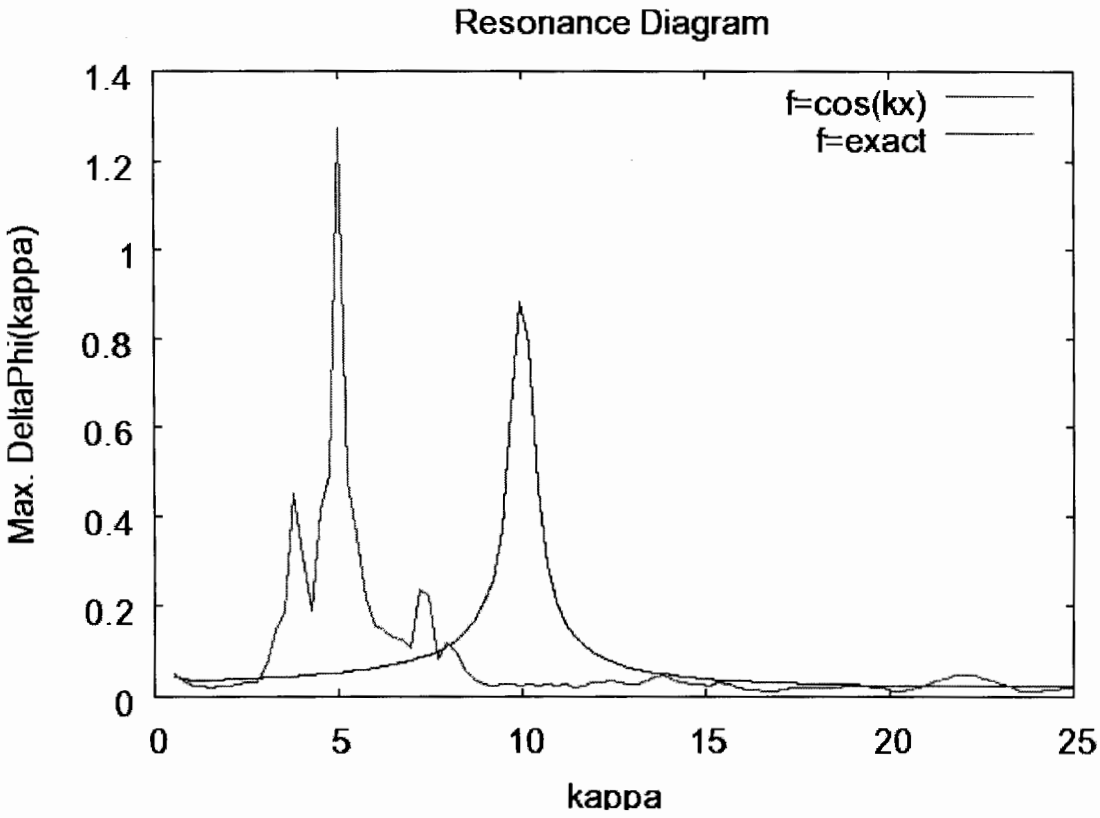

Fig. 15. Resonance diagram, max. amplitude after 15 wavelengths $\lambda=2\pi/\kappa$.

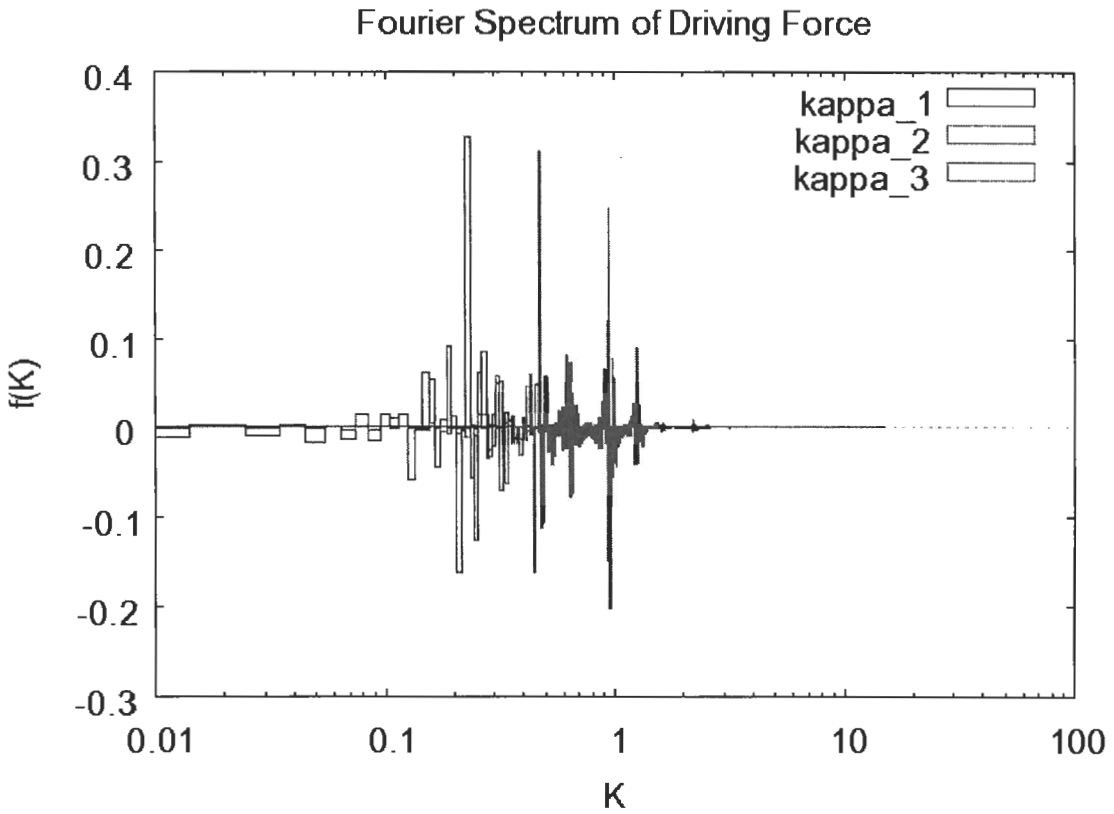

Fig. 16. Fourier transform of driving force for three wave numbers (2.5, 5, 10).

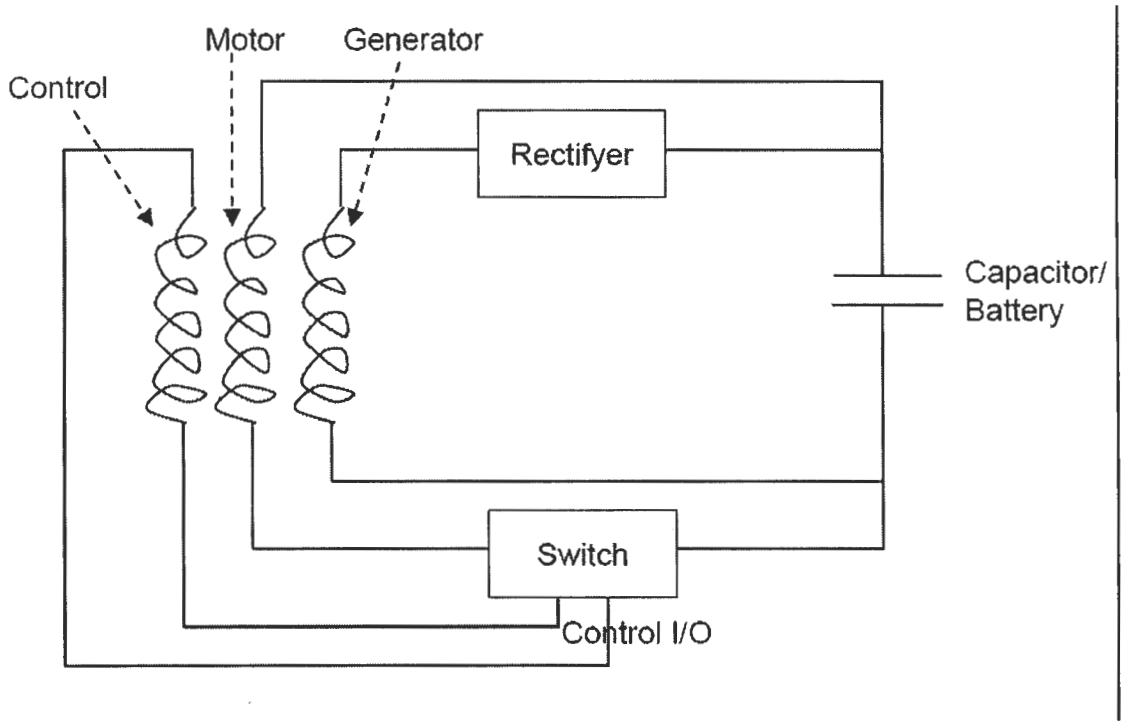

Fig. 17. Block diagram of Bedini motor-generator.